Multiphoton microscopy based on four-wave mixing of colloidal quantum dots

Francesco Masia, Wolfgang Langbein, and Paola Borri[a)]
School of Physics and Astronomy and School of Biosciences, Cardiff University, The Parade, Cardiff CF24 3AA, United Kingdom

(Received 11 June 2008; accepted 27 June 2008; published online 16 July 2008)

We demonstrate a novel multiphoton imaging modality based on the detection of four-wave mixing (FWM) from colloidal nanoparticles. This third-order signal is excited and detected in resonance with the ground-state excitonic transition of CdSe/ZnS quantum dots. We measure transversal and axial resolutions of 140 and 590 nm, respectively, significantly improved compared to the one-photon diffraction limit. The coherent FWM signal is detected using a heterodyne technique which rejects incoherent background for improved image contrast compared to fluorescence methods. As sensitivity limit, we estimate a minimum number of 10 dots/$\sqrt{\text{Hz}}$ detectable in the focal volume. © *2008 American Institute of Physics*. [DOI: 10.1063/1.2959737]

Optical microscopy is an indispensable tool that is driving progress in cell biology, and is still the only practical means of obtaining spatial and temporal resolution within living cells and tissues. Much effort is being devoted recently to achieve high three-dimensional (3D) spatial resolution in fluorescence microscopy by exploiting nonlinear effects. In multiphoton fluorescence, fluorophore excitation occurs by the simultaneous absorption of two[1] or three[2] photons which can only take place in the focal volume where high photon densities are reached, thus resulting in an intrinsic 3D resolution. Very recently, new strategies have been developed to achieve nanometric spatial resolution (10–100 nm) overcoming the classical diffraction limit via saturation effects such as in stimulated emission depletion microscopy.[3]

Advances in the chemical synthesis of colloidal quantum dots (CQDs) have allowed fabrication of water-soluble and biocompatible nanocrystals generating widespread interest as novel inorganic luminescent probes.[4] CQDs have unique optical properties compared to organic fluorophores, such as broad and strong absorption spectra, narrow emission bands, and size-dependent emission wavelengths. Moreover, they appear to be much more photostable, have luminescence lifetimes (10–100 ns) significantly longer than organic fluorophores (0.1–4 ns), and also exhibit large two-photon absorption cross sections.[5]

Although not yet explored for multiphoton imaging to date, it is known since many years that CQDs also exhibit a large third-order optical nonlinearity, resulting in four-wave mixing (FWM), when excited in resonance with their fundamental excitonic transition.[6] In a two-beam transient FWM experiment,[7] the optical field E_1 of a first pulse generates a coherent polarization in the sample which is converted into a third-order polarization $\propto E_1^* E_2^2$ by the field E_2 of a second pulse, typically due to absorption bleaching by the carrier density $\propto E_1^* E_2$.

In this work, we demonstrate that resonant FWM from CQDs can be used as a novel multiphoton imaging modality with higher spatial resolution and optical sectioning capabilities than two-photon fluorescence (TPF). The investigated sample consisted of commercially available trioctylphosphine-oxide-capped CdSe/ZnS CQDs dots (Plasmachem GmbH) dispersed in a polymethylmethacrylate (PMMA) and toluene solution (final CQD concentration 10 μM) and spin coated on a 0.17 mm thick glass coverslip. In these CQDs, we measured a photoluminescence (PL) quantum yield of 40% and an emission spectrum at room temperature centered at 610 nm with 33 nm linewidth full width at half maximum (FWHM) due to a combination of homogeneous and inhomogeneous broadening. Single CQD PL spectra showed a homogeneous linewidth of ~20 nm at room temperature.[8] As optical excitation, we used Fourier-limited laser pulses of 150 fs duration (~4 nm spectral width) at 76 MHz repetition rate with a center wavelength tunable from 550 to 700 nm, provided by the intracavity frequency doubled signal of an optical parametric oscillator pumped by a Ti:sapphire laser. The experiment is performed using a modified version of the transient FWM in heterodyne detection demonstrated in our previous works.[9,10] In this experiment (see Fig. 1) the two exciting pulses ($P_{1,2}$) are frequency upshifted by a radio-frequency amount ($\nu_{1,2}$) using acousto-optic modulators and, after being recombined in a beam splitter, focused into the sample by an oil-immersion microscope objective (MO) with 1.25 numerical aperture (NA) to achieve high spatial resolution. 3D sample scanning is realized by a piezoelectric

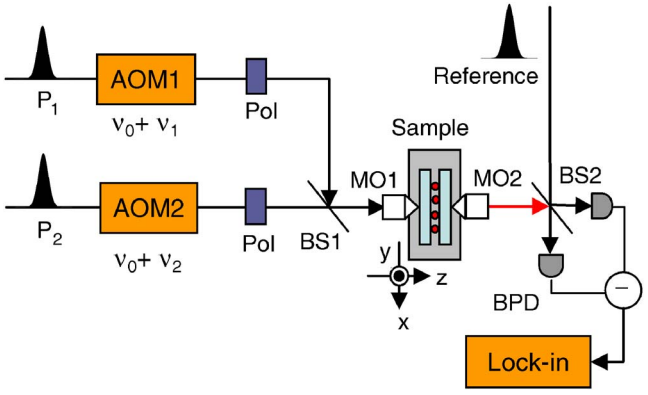

FIG. 1. (Color online) Sketch of the experimental setup. AOM: acousto-optic modulator, pol: polarization control, *xyz*: piezoelectric scanning stage, BS: 50:50 beam splitter, MO: microscope objective, and BPD: balanced photodiodes.

[a)]Electronic mail: borrip@cardiff.ac.uk.

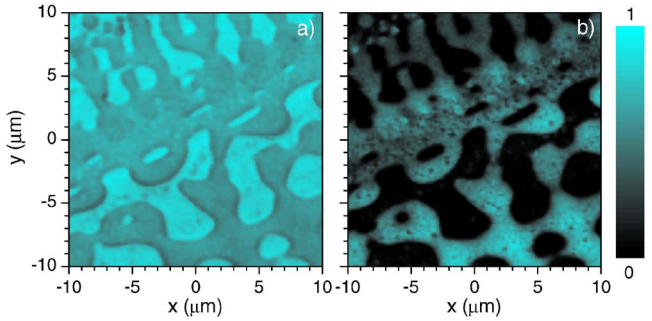

FIG. 2. (Color online) (a) Transmitted intensity of P_2 as a function of the transverse position of the sample. (b) FWM intensity of the same region. Linear color scale as given. The excitation wavelength is 590 nm and the excitation intensity in the focus 16 kW/cm^2. The pixel size is 0.2 $\times$0.2 μm^2 and the integration time per pixel is 50 ms.

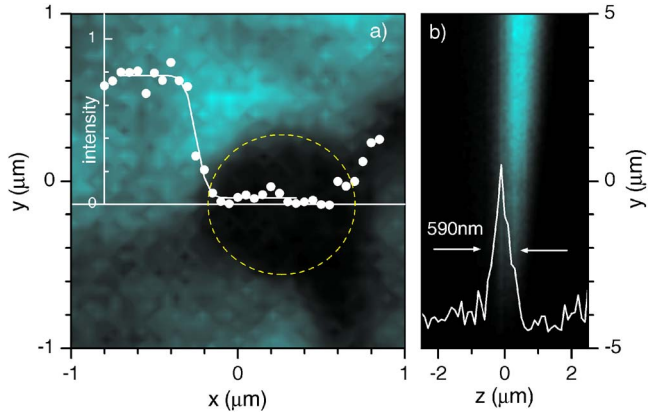

FIG. 3. (Color online) (a) FWM intensity xy scan. Linear color scale as in Fig. 2. The intensity along the x cut indicated by the horizontal line is shown (circles) together with a fit. The pixel size is 50$\times$50 nm^2, the integration time per pixel is 50 ms, and the excitation intensity is 12 kW/cm^2. (b) Normalized FWM intensity yz scan. Axial profile of the intensity is shown for y=−4.1 μm. The pixel size is 0.1$\times$0.1 μm^2 the integration time per pixel is 50 ms and the excitation intensity is 45 kW/cm^2.

scanning unit with nanometric resolution (Physik Instrumente PI F-130). The transmitted fields of $P_{1,2}$ and the FWM signal are collected by a second MO, and the interference with an unshifted reference beam in the beam splitter BS2 is detected by a pair of balanced photodiodes and a lock-in amplifier, at the appropriate beating radio frequency (e.g., $2\nu_2-\nu_1$ for the FWM). The polarization states of $P_{1,2}$ are adjusted by a combination of $\lambda/4$ and $\lambda/2$ waveplates. P_1 is cross polarized with respect to the reference, to minimize interference in the photodiodes, while the polarization of P_2 is chosen to maximize the detected FWM signal. The measured homogeneous linewidth of the fundamental exciton transition in the CQDs at room temperature corresponds to a dephasing time of the induced polarization of ~20 fs, smaller than the pulse duration. Hence, we have adjusted the delay time between P_1 and P_2 to time overlap in order to optimize the FWM signal.

Figure 2(a) shows the transmitted intensity of P_2 as a function of the transverse position of the sample in a xy scan. The total time-averaged incident intensity in the focus was $\bar{I}\sim 16$ kW/cm^2 and the pulse spectra were centered on the CQD absorption peak at 590 nm. Darker regions correspond to areas with lower transmission, indicating a high concentration of CQDs, while brighter regions correspond to the absence of CQDs in the volume, as was also confirmed by widefield epifluorescence. The corresponding FWM intensity of the same region [Fig. 2(b)] vanishes at the positions of maximum transmission, and is maximum for minimum transmission, as expected. The FWM image contrast is high, with the maximum FWM intensity being three orders of magnitude above the background. Note that compared to fluorescence detection, such coherent FWM signal detected interferometrically is free from any incoherent (e.g., autofluorescence, Raman) background.

Because of the third-order nonlinear nature of the FWM signal, an improved spatial resolution beyond the one-photon diffraction limit is expected. To determine the transversal spatial resolution of this FWM microscopy, we dispersed silica beads into the CQDs/PMMA/toluene solution prior to spin coating. These beads create volumes of zero CQD concentration and sharp edges, embedded in the surrounding medium of high CQD concentration. Figure 3(a) shows the FWM intensity as a function of the transverse position in a xy scan over the sample where the silica beads are dispersed. The volume with low intensity (black) reveals the presence of a silica bead of ~1 μm diameter (dashed circle). The measured FWM intensity along the x direction defined by the horizontal line is constant on the left of the bead, from which a homogeneous QD distribution can be deduced. The FWM intensity profile is therefore determined by the convolution of the instrumental intensity point spread function (PSF) and the step profile of the CQD concentration. For a Gaussian PSF, the resulting profile is given by $S(x)\propto 1-\mathrm{erf}[(x-x_0)/(\sqrt{2}\sigma)]$, where σ is the standard deviation of the Gaussian PSF connected to its FWHM by $\sigma\sqrt{8\ln 2}$. A fit to the data [solid line in Fig. 3(a)] yields a FWHM of ~140 nm.[11] For comparison, the diffraction limit can be calculated for the same excitation wavelength λ=590 nm and objective NA=1.25 using the FWHM of the transversal PSF $I_t=[2J_1(v)/v]^2$ given by the one-photon intensity distribution at the focus, where J_1 is the first-order Bessel function and $v=2\pi x\mathrm{NA}/\lambda$, which results in 240 nm transversal resolution. For an ideal confocal microscope,[12] the FWHM of the function I_t^2 leads to a transversal resolution of 174 nm. This assumes a pinhole of negligible diameter, while for realistic diameters the resolution deteriorates by ~25%. For a TPF microscope which utilizes an excitation wavelength twice as large, the transversal resolution is 348 nm. Therefore, the transversal resolution of our FWM microscope is not only beyond diffraction limit, but also surpasses that of a confocal and a two-photon microscope.

We have measured the axial resolution, and thus the optical sectioning capability of our technique, by quantifying the FWHM of the FWM intensity profile along the z direction in a sample where a solution of CQDs/toluene was drop cast on a coverslip. A yz scan of the FWM intensity at the edge of the drop is shown in Fig. 3(b). The intensity profile along the axial direction has a width which increases toward the center of the drop, tracing its thickness. This intensity profile is given by the convolution of the axial PSF and the CQD distribution. For a local drop thickness much smaller than the axial resolution, the intensity FWHM is dominated by the PSF. We measured an intensity FWHM of 590 nm [see Fig. 3(b)], which can be considered as an upper limit of the axial resolution of the technique. The measured value is below the FWHM of the one-photon on-axis PSF given by $I_a=[\sin(u/4)/(u/4)]^2$, where $u=2\pi z\mathrm{NA}^2/(\lambda n)$ (with n

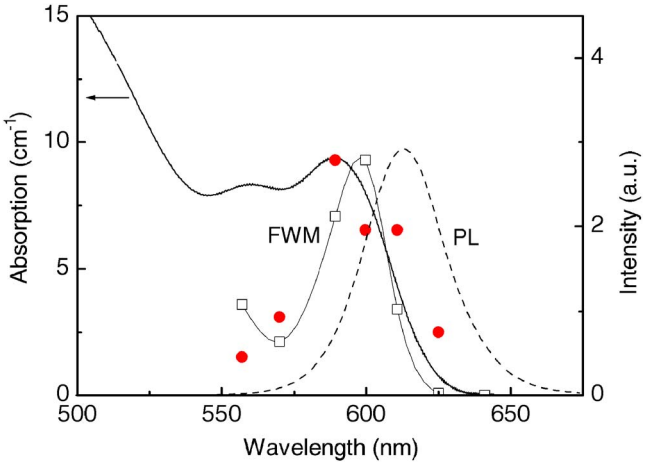

FIG. 4. (Color online) FWM efficiency in the low excitation power regime (open squares) and in the excitation regime corresponding to the maximum emitted FWM intensity (circles) as a function of excitation wavelength. The normalized PL spectrum and the absorption coefficient of 10 μM CQDs are also shown.

=1.51 refractive index of oil), which results in 1010 nm axial resolution in the presence of a pointlike object [while for a planar structure such as in Fig. 3(b), the one-photon function would have no axial resolution]. In an ideal confocal fluorescence microscope[12] the FWHM of I_t^2 gives an axial resolution of 730 nm, and for a TPF microscope with $\lambda_{TPA}=2\lambda$ the resolution would be 1460 nm. Also in this case, the axial resolution of our FWM microscope is significantly better.

For a total intensity in the focus $\bar{I}<0.03$ MW/cm^2, the FWM field amplitude scales with the intensities of P_1 and P_2 as expected from a third-order nonlinearity. In this regime, the ratio between the intensities of P_1 and P_2 for which the largest FWM signal is created for a given total excitation intensity is 0.5, as expected.[7] At higher excitation intensities, the FWM deviates from the third-order scaling due to a saturation of the exciton density in the CQDs. A saturation of the FWM signal and of the absorption bleaching is measured for $\bar{I}\sim 5$ MW/cm^2. Increasing the intensity above this level leads to an irreversible damage of the sample. From the maximum emitted FWM at saturation we have estimated the sensitivity of the technique. The detected FWM field amplitude is proportional to the number of CQDs in the focal volume (calculated from the measured attenuated transmission and the known extinction coefficient and transversal focus area) from which we deduce the maximum FWM amplitude per single CQD. The measured amplitude noise in the detection for a given bandwidth is due to the shot noise of the reference and is found to be equivalent to the maximum amplitude from 10 CQDs/$\sqrt{\text{Hz}}$ detection bandwidth.

We have characterized the spectral dependence of the FWM response by measuring the emitted FWM intensity as a function of the excitation wavelength. In Fig. 4 the absorption and PL spectra of the investigated CdSe/ZnS CQDs are shown and compared to the measured FWM efficiency (open squares) for different excitation wavelengths in the low excitation power regime. The FWM efficiency is obtained by dividing the detected FWM intensity by the intensity of P_1 and the square of the intensity of P_2, according to the third-order nonlinearity. The FWM efficiency shows its maximum near the ground-state excitonic absorption peak, while it is significantly reduced for excitation near the first excited state even if the absorption is essentially constant in this range, possibly due to a reduced oscillator strength[13] and/or a faster dephasing of these excited states. The maximum emitted FWM intensity (for high excitation power) is also shown in Fig. 4 (circles). In this case, we observe a broader spectral dependence indicating a less resonant behavior of the polarization which is expected at saturation. From the point of view of practical applications, these results show that multicolor FWM imaging is possible with CQDs of different sizes and/or compositions, thus having different ground-state excitonic FWM resonances that can be used to selectively tag different parts of the specimen.

Considering the growing commercial availablility of CQD-biomolecule conjugates, this new imaging modality could be readily applied to cell microscopy offering increased spatial resolution and autofluorescence background-free detection. Such FWM imaging is also applicable to CQDs emitting in the near infrared for deeper penetration in tissues since the heterodyne detection does not suffer from the high dark noise of detectors in this wavelength range. Beyond CQDs, this technique would also operate with nonfluorescent labels yet exhibiting high oscillator strengths and third-order optical nonlinearities such as metallic nanoparticles.

The authors acknowledge the UK Engineering and Physical Sciences Research Council for financial support (Grant No. EP/E0131198/1).

[1]W. Denk, J. H. Strickler, and W. W. Webb, Science **248**, 73 (1990).
[2]S. W. Hell, K. Bahlmann, M. Schrader, A. Soini, H. M. Malak, I. Gryczynski, and J. R. Lakowicz, J. Biomed. Opt. **1**, 71 (1996).
[3]S. W. Hell, Science **316**, 1153 (2007).
[4]A. P. Alivisatos, W. Gu, and C. Larabell, Annu. Rev. Biomed. Eng. **7**, 55 (2005).
[5]D. R. Larson, W. R. Zipfel, R. M. Williams, S. W. Clark, M. P. Bruchez, F. W. Wise, and W. W. Webb, Science **300**, 1434 (2003).
[6]D. M. Mittleman, R. W. Schoenlein, J. J. Shiang, V. L. Colvin, A. P. Alivisatos, and C. V. Shank, Phys. Rev. B **49**, 14435 (1994).
[7]J. Shah, *Ultrafast Spectroscopy of Semiconductors and Semiconductor Nanostructures* (Springer, Berlin, 1996).
[8]Y. Sun, F. Masia, W. Langbein, and P. Borri, Phys. Status Solidi B (unpublished).
[9]P. Borri and W. Langbein, J. Phys.: Condens. Matter **19**, 295201 (2007).
[10]P. Borri, W. Langbein, S. Schneider, U. Woggon, R. L. Sellin, D. Ouyang, and D. Bimberg, Phys. Rev. Lett. **87**, 157401 (2001).
[11]Since the image originates from a linear superposition of FWM fields, rather than intensities, the PSF should actually be defined in the signal field. We have checked the PSF in the FWM amplitude data and found a transversal and axial FWHM of ~190 and ~810 nm, respectively, which, assuming a gaussian response function, correspond to a FWHM of the intensity PSF of 135 and 570 nm.
[12]M. Müller, *Introduction to Confocal Fluorescence Microscopy* (SPIE, Bellingham, Washington, 2006).
[13]U. E. H. Laheld and G. T. Einevoll, Phys. Rev. B **55**, 5184 (1997).